Tellus (2005), 57A, 758–769
Printed in Singapore. All rights reserved

TELLUS

Westward propagation of the Indian monsoon depression

By TSING-CHANG CHEN*, JIN-HO YOON and SHIH-YU WANG, *Atmospheric Science Program, Department of Geological and Atmospheric Sciences 3010 Agronomy Hall, Iowa State University, Ames, Iowa 50011, USA*

(Manuscript received 26 July 2004; in final form 10 February 2005)

ABSTRACT

Being restricted in their vertical development by the Tibetan high, monsoon depressions propagate westward against monsoon westerlies embedded in the Indian monsoon trough. The cause of this peculiar propagation has not been well explained. Special characteristics of individual depressions were revealed from observations of previous studies; particularly, the major rainfall of a depression occurs over its west–south-west sector. The latent heat released by this rainfall forms east–west differential heating across the depression in developing an east–west asymmetric circulation. Because this east–west circulation is a part of the depression's divergent circulation, a spatial quadrature relationship exists between this divergent circulation and the depression. Based on these characteristics, a westward propagation mechanism of the depression is introduced. The depression's rainfall is supported by the convergence of water vapor transported by the low-level divergent circulation. In turn, the divergent circulation is maintained through a feedback of the latent heat released by the rainfall. The upward branch of the east–west circulation coupled with the convergent center of the low-level divergent circulation generates a negative streamfunction tendency. The depression is propagated westward by a dynamic interaction between rainfall/convection and this monsoon disturbance through the negative streamfunction tendency. The spatial quadrature relationship between a depression and its east–west (divergent) circulation rejuvenates the water vapor supply maintaining diabatic heating and the divergent circulation, and perpetuating the generation of negative streamfunction tendency ahead of the depression. The entire process from the maintenance of east–west differential heating to the generation of negative streamfunction tendency west of a depression will not diminish until the cessation of water vapor supply.

Budget analyses of heat, water vapor, velocity potential, and streamfunction for 143 depressions identified over 24 summers (1979–2002) were performed with ERA-40 reanalyses and three daily rainfall data sources. The westward propagation mechanism of monsoon depressions was illustrated/confirmed in terms of these budget analyses.

1. Introduction

The Indian monsoon consists of the Tibetan high in the upper troposphere and the Indian monsoon trough in the lower troposphere. The vertical development of depressions is thus restricted below 300 mb by the Tibetan high (Sikka, 1977; Chen and Yoon, 2000). The westward propagation of monsoon depressions takes place not only underneath the Tibetan high, but also against monsoon westerlies. Prevailing winds in the mid-latitudes are westerlies, while atmospheric flows in the tropics are primarily easterlies. Therefore, extratropical synoptic cyclones propagate eastward ahead of upper-level short-wave troughs by advection of strong westerlies and tropical synoptic disturbances – including easterly waves in the Caribbean Sea (Riehl, 1954), equatorial waves in the western tropical Pacific (Palmer, 1952; Yanai et al., 1968; Reed and Recker, 1971), and African easterly waves in West Africa (Carlson, 1969a,b; Burpee, 1972) – propagate westward by advection of strong easterlies. The contrast of propagation direction between extratropical cyclones/tropical synoptic disturbances and monsoon depressions implies that the horizontal advection by environmental flow is crucial to the propagation direction of the former synoptic disturbances, but not important to the latter depressions. The peculiar propagation property of monsoon depressions leads us to search for their propagation mechanism.

Based on the linear wave theory developed on the tropical beta plane by Matsuno (1966), Krishnamurti et al. (1977) suggested that the westward propagation of a monsoon depression might be due to the downstream amplification of the westward propagating Rossby-like wave with a phase speed about three times the westward propagating group velocity. The basic flow

*Corresponding author.
e-mail: tmchen@iastate.edu

used by Krishnamurti et al. was zonal-mean easterly of 2.7 m s^{-1}. As revealed from the July-mean zonal wind cross-section between the equator and 25°N at 85°E, shown by Shukla (1978), the upper-tropospheric monsoon easterlies in the Indian monsoon region yield to the lower-tropospheric monsoon westerlies below 400 mb. These monsoon westerlies can have peak speeds of 15 m s^{-1}. Because of the limited vertical extent of the monsoon depression and the vertical structure of zonal flow in northern India and the Bay of Bengal, the upper-level tropical easterlies do not seem to play any significant role in transporting monsoon depressions westward (Chen and Yoon, 2000). Actually, the westward propagation of a monsoon depression against the prevailing monsoon westerlies below 400 mb is a peculiar behavior.

Examining the heat budget of a MONEX (Monsoon Experiment) depression, Saha and Saha (1988) argued that the latent heat released by cumulus convection/rainfall in the west–south-west sector of this depression sustained an upward branch of the east–west asymmetric circulation across a depression with a downward branch east of the depression center. It was suggested by Daggupaty and Sikka (1977), based on the vorticity budget analysis, and by Sanders (1984), from his quasi-geostrophic streamfunction budget analysis, that the westward movement of a depression may be caused by imbalance between vorticity advection and vortex stretching. Analyzing the detailed streamfunction budget analysis of another MONEX monsoon depression, Chen and Yoon (2000) showed that the negative streamfunction tendency induced by the upward branch of the east–west circulation may move the depression westward. Therefore, they suggested that the westward propagation of a monsoon depression is a dynamic response of the depression to the coupling of the conditional instability of second kind (CISK) mechanism with the east–west circulation of this depression. However, two important components of this mechanism were missing from previous studies.

(i) How is water vapor supplied to maintain cumulus convection/rainfall over the west–south-west sector of a depression? An extensive water budget analysis of 143 monsoon depressions over the period 1979–2002 was performed in a recent study of Yoon and Chen (2005). It was shown that water vapor was converged toward the west–south-west sector of a monsoon depression by its divergent circulation to support rainfall over its west–south-west sector. However, the coupling of the divergent circulation with the westward propagating monsoon depression was not clear.

(ii) The east–west circulation is driven/maintained by the latent heat released from the rainfall over the west–south-west sector of a depression. Because the east–west circulation is a part of the depression's divergent circulation, how is this divergent circulation coupled with diabatic heating?

Based on budget analyses of heat, water vapor, and streamfunction of previous studies and the two aforementioned missing components, a westward propagation mechanism of the monsoon depression is proposed in Section 2. In order to illustrate this mechanism, several types of data were used in this study and are presented in Section 3: the ERA-40 reanalysis data (Källberg et al., 2004) for the period 1979–2002, and three different precipitation data sets covering different periods between 1979 and 2002 were applied to all depressions identified over 24 summers. Composite budgets of the previous three variables and velocity potential were performed. Results of these budget analyses are synthesized in Section 4 to substantiate the proposed mechanism. Concluding remarks are offered in Section 5.

2. Propagation mechanism

It was hypothesized that the westward propagation of a monsoon depression was caused by a coupling of the asymmetric circulation across the depression with the CISK mechanism. This mechanism will be elucidated by the synthesis of simplified budget analyses of heat, water vapor, velocity potential, and streamfunction.

According to their heat budget of a MONEX monsoon depression (3–8 July 1979), Saha and Saha (1988) showed that the local rate of change of temperature ($\partial T/\partial t$) and thermal advection ($-\mathbf{V}\cdot\nabla T$) of this depression during its mature stage were generally much smaller in magnitude than diabatic warming ($-\sigma\omega$) and diabatic heating ($\dot{\mathbf{Q}}/c_p$). Generally, heating appears over the west/south-west sector of a monsoon depression where heavy rainfall occurs, and cooling is present over the east/north-east sector. After tedious heat budget analyses of 143 monsoon depressions, we obtained the same outcome. In other words, the heat budget equation (its complete form is eq. A1 in Appendix A) may be approximated by the following form

$$-\sigma\omega \simeq \dot{\mathbf{Q}}/c_p, \tag{1}$$

not only for the deep convection over the west/south-west sector, but also for the diabatic cooling area over the east/north-east sector of a monsoon depression. Symbols used in all equations hereafter are explained in Table 1.

Vertical motion is part of the atmospheric divergent circulation (which is often portrayed by velocity potential χ), while horizontal divergence ($\nabla\cdot\mathbf{V}$) can be expressed in terms of the Laplacian of velocity potential, i.e. $\nabla\cdot\mathbf{V} = \nabla^2\chi$. Combining eq. (1) with the continuity equation

$$\nabla\cdot\mathbf{V} + \frac{\partial\omega}{\partial p} = 0$$

and replacing divergence by velocity potential, one can easily obtain the simplified χ-maintenance equation (its complete form is eq. A2 in Appendix A):

$$\chi \simeq \nabla^{-2}\left[\frac{\partial}{\partial p}\left(\frac{1}{\sigma c_p}\dot{\mathbf{Q}}\right)\right] = \chi_{\dot{Q}}. \tag{2}$$

Evidently, a divergent circulation can be maintained by diabatic heating ($\dot{\mathbf{Q}}/c_p$) through vertical motion with the relationship

Table 1. List of symbols

Symbol	Meaning
T	temperature
W	precipitatable water $\equiv (1/g)\int_0^{p_s} q\,\mathrm{d}p$
χ	velocity potential
ψ	streamfunction
$\mathbf{V}$	wind vector
σ	static stability
c_p	specific heat capacity with constant pressure
ω	p vertical velocity $\equiv (\mathrm{d}p/\mathrm{d}t)$
$\dot{\mathbf{Q}}$	diabatic heating
$\mathbf{Q}$	water vapor flux $\equiv (1/g)\int_0^{p_s} (\mathbf{V}q)\,\mathrm{d}p$
q	specific humidity
p, p_s	pressure, surface pressure
E	evaporation
P	precipitation
ζ	vorticity
f	Coriolis parameter

shown in eq. (1). The east–west circulation across a monsoon depression is depicted by (u_D, $-\omega$), in which u_D is divergent zonal motion and can be related to diabatic heating through the following relation:

$$u_D\left(=\frac{\partial\chi}{\partial x}\right)=\nabla^{-2}\left[\frac{\partial}{\partial p}\left(\frac{1}{\sigma c_p}\frac{\partial\dot{\mathbf{Q}}}{\partial x}\right)\right].$$

It is revealed from this relationship that the east–west asymmetric circulation of a depression is driven by east–west differential heating

$$\frac{1}{c_p}\frac{\partial\dot{\mathbf{Q}}}{\partial x}.$$

The diabatic heating of a depression is primarily (∼80%) contributed through the latent heat released from rainfall over its west–south-west sector (Saha and Saha, 1988). How is this depression's rainfall maintained? This question can be answered through the water vapor budget (its complete form is referred to by eq. A3 in Appendix A) of a depression. A comprehensive analysis of all 143 identified monsoon depressions was performed by Yoon and Chen (2005). It was shown that the local rate change of precipitable water (i.e. storage term $\partial W/\partial t$) is small compared to other terms in the depression water budget. Although evaporation (E) is not observed, it is possible to estimate it in terms of a residual method of the water vapor equation:

$$E=\frac{\partial W}{\partial t}+\nabla\cdot\mathbf{Q}+P.$$

However, this estimation may include bias of the data assimilation system and computational errors. As observed by Yoon and Chen (2005), the major water vapor supply to maintain a depression's rainfall is largely accomplished through the convergence of water vapor flux ($\nabla\cdot\mathbf{Q}$). This hydrological relationship may be expressed as

$$P\sim-\nabla\cdot\mathbf{Q}. \tag{3}$$

Rainfall, which is a local hydrological process, is maintained by the local convergence of water vapor flux (eq. 3). In order to link this local process with the large-scale circulation, Chen (1985) introduced the potential function of water vapor flux, χ_Q. This hydrological process may be expressed as

$$\chi_Q\sim\nabla^{-2}(-\mathrm{P}). \tag{4}$$

Because the majority of precipitable water resides in the lower troposphere, water vapor transport is primarily carried out by the lower-tropospheric circulation. It is expected that spatial patterns of χ_Q and lower-tropospheric χ are similar. It is inferred from the comparison between eqs. (2) and (4) that the divergent circulation is maintained by the latent heat released from rainfall. This is also true of the east–west asymmetric circulation of monsoon depressions.

How is a monsoon depression propagated by the east–west circulation? This fundamental question will be answered by analysis of the streamfunction budget:

$$\underset{\psi_t}{\nabla^{-2}\left(\frac{\partial\zeta}{\partial t}\right)}=\underset{\psi_A}{\nabla^{-2}[-\mathbf{V}\cdot\nabla(\zeta+f)]}+\underset{\psi_\chi.}{\nabla^{-2}[-(\zeta+f)\nabla\cdot\mathbf{V}]} \tag{5}$$

Sanders (1984) analyzed the streamfunction budget of the 5–8 July 1979 MONEX monsoon depression, while Chen and Yoon (2000) analyzed the 19–25 June 1979 MONEX monsoon depression. It was shown by Krishnamurti et al. (1977) that the spatial structure of monsoon depressions could be properly depicted by the short-wave (6–25) regime. A variable ( ) in this wave regime can be denoted by $(\,)^s$. Previous budget analysis showed that ψ_A^s was much smaller in magnitude than ψ_χ^s (Sanders, 1984; Chen and Yoon, 2000). Therefore, the streamfunction budget of a depression may be expressed by the following approximation of eq. (5):

$$\psi_t^s\sim\psi_\chi^s. \tag{6}$$

It is inferred from this equation that the negative streamfunction tendency can be generated over the west–south-west sector of a monsoon depression through vortex stretching by the upward branch of the depression's east–west asymmetric circulation. Because monsoon depressions generally propagate westward along the Indian monsoon trough, the total vorticity ($\eta=\zeta+f$) of these depressions is always cyclonic. In order to facilitate our discussion, let us assume that η associated with vortex stretching in eq. (5) is constant. We may then approximate eq. (6) as

$$\psi_t^s\sim-\eta\chi^s. \tag{7}$$

Two important implications of the depression's development may be derived from eqs. (6) and (7): westward propagation of a monsoon depression, and coupling between a monsoon depression and its east–west circulation.

Recall that $\zeta = \nabla^2\psi$ and $\nabla \cdot \mathbf{V} = \nabla^2\chi$. If ψ and χ are expressed in terms of sinusoidal functions, we may write them as

$$\psi = \sum_{n=0}^{N} \psi^n e^{i(n\lambda - \nu t)} \quad \text{and} \quad \chi = \sum_{n=0}^{N} \chi^n e^{i(n\lambda - \nu t)},$$

respectively, where $(\,)^n$ represents the wavenumber n component of $(\,)$. For the short-wave regime, these two variables may be written as

$$\psi^s = \sum_{n=6}^{25} \psi^n e^{i(n\lambda - \nu t)} \quad \text{and} \quad \chi^s = \sum_{n=6}^{25} \chi^n e^{i(n\lambda - \nu t)},$$

and eq. (7) as the following form:

$$\sum_{n=6}^{25} \psi_t^n \sim \sum_{n=6}^{25} -\eta\chi^n. \tag{8}$$

As indicated by this equation, streamfunction tendency should be out of phase with the divergent circulation depicted by velocity potential. It is shown by the schematic diagram in Fig. 1 that the convergent center of the east–west circulation west of a depression center overlaps the negative streamfunction tendency. Therefore, the depression is propagated westward by this negative tendency.

Equation (6) may be expressed in a different form:

$$\sum_{n=6}^{25} \psi^n \sim \sum_{n=6}^{25} \frac{\eta}{\nu n^2} \chi^n e^{-i(\pi/2)}. \tag{9}$$

It is indicated by the factor $e^{-i(\pi/2)}$ that ψ^n and χ^n are spatially in quadrature; negative anomalies of ψ^n are located west of negative χ^n anomalies. Based on this argument, the ψ^s–χ^s spatial relationship is shown in Fig. 1. In order to maintain this spatial relation, a westward propagating depression ($\psi^s < 0$) by the negative streamfunction tendency ($\psi_t^s < 0$) requires a response of the divergent circulation coupled with the depression to satisfy eq. (9). The convergence of water vapor toward the convergent center ($\chi^s > 0$) west–south-west of the moving depression follows the response of the divergent circulation to support the accompanying rainfall and the latent heat released from rainfall through a CISK mechanism. The depression is propagated westward by the coupling between the CISK and dynamic ψ^s–χ^s interaction. These processes will not be terminated until the water vapor supply to maintain the depression's rainfall diminishes.

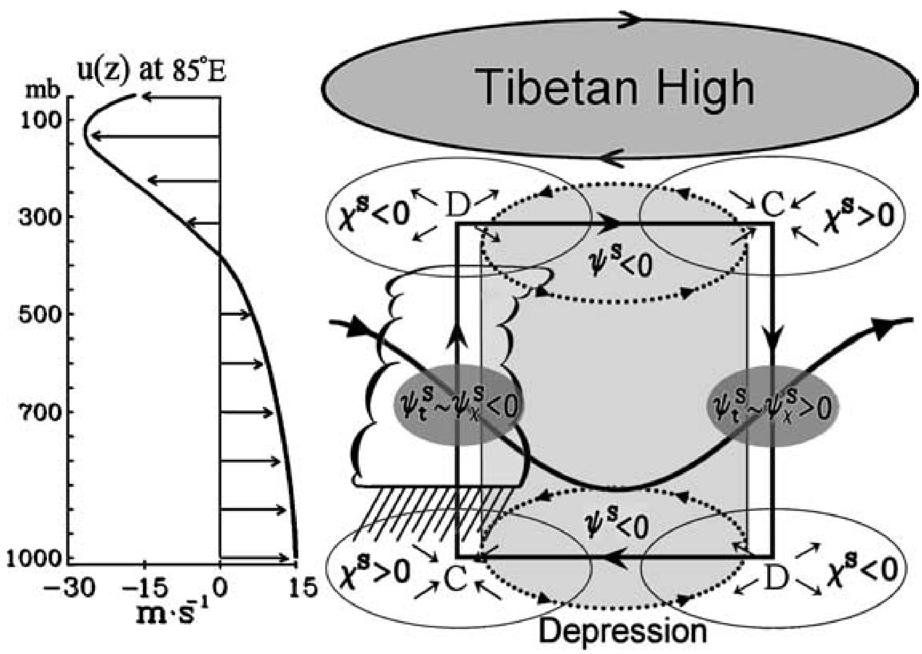

Fig. 1. A schematic diagram depicting the westward propagation mechanism of a monsoon depression ($\psi^s < 0$) embedded in the lower-tropospheric monsoon westerlies (indicated by the left diagram) and overlaid by the Tibetan high (the elliptic stippled area at the top of the right diagram). The combination of the depression and monsoon westerlies is portrayed by the thick sinusoidal streamline. The east–west asymmetric circulation of the depression is denoted by solid lines with shafts encircling this depression, which is represented by the stippled cylinder. The divergent circulation (χ^s) coupled with the east–west circulation is denoted by thin-line circles centered at Ds and Cs at the upper and lower levels. Cumulus convection/rainfall west of the depression center is coincident with the upward branch of the east–west circulation. This depression is moved westward by the negative (positive) streamfunction tendency (ψ_t^s) generated by the vortex stretching (ψ_χ^s) associated with the upward (downward) branch of the east–west circulation.

3. Data and analysis

The data used in this study include reanalysis, precipitation (P), vertical motion (ω), and diabatic heating ($\dot{Q}$). The life cycle of a monsoon depression may range from 3 to 6 d. We portray this life cycle in terms of ERA-40 reanalyses (Källberg et al., 2004) twice a day (00 and 12 UTC) for the period of 1979–2002. These data were used to identify the monsoon depression and to perform four different (heat, water vapor, velocity potential, and streamfunction) budget analyses. The identification scheme of monsoon depressions used by Chen and Weng (1999) was adopted by Yoon and Chen (2005). In total, 143 monsoon depressions were identified by Yoon and Chen (2005) over 24 summers (1979–2002). As observed by previous studies (e.g. Saha et al., 1981; Chen and Weng, 1999), six monsoon depressions propagate into the Indian subcontinent every monsoon season. Budget analyses of four different variables will be applied to elucidate the proposed propagation mechanism of monsoon depressions.

The depiction of the hydrological processes of monsoon depressions needs several hydrological variables: winds, water vapor, precipitation, and evaporation. The first two variables were directly supplied by the ERA-40 reanalysis. Because precipitation and evaporation were not initially specified in the data assimilation cycle, they were generated by the model. In other words, these two hydrological variables were not obtained from observations and might contain bias of the data assimilation system. Currently, there are three sets of daily global precipitation available: the Global Precipitation Climatology Project (GPCP; Huffman et al., 1997), the Tropical Rainfall Measuring Mission (TRMM; Simpson et al., 1988), and the Goddard Precipitation estimation (called GPI; Susskind et al., 1997). However, the first two precipitation data sets cover a period of only 5 yr (1997–2002). The precipitation estimations generated with satellite infrared (IR) observations by Susskind et al. (1997) of the Goddard Space Flight Center may be used as an alternative. This precipitation proxy (GPI) provides a daily data set for two periods (1979–1980 and 1986–1997) with a $1^\circ \times 1^\circ$ resolution. Being essentially an oceanic rainfall proxy, the GPI may contain some bias over land. To avoid this potential problem, station rainfall observations over India archived at the National Center for Atmospheric Research were interpolated into a $1^\circ \times 1^\circ$ mesh with the Cressman (1957) scheme and merged with GPI. For details of this merger, refer to Yoon and Chen (2005). Rainfall of all identified depressions during the time periods of rainfall available will be used to prepare composite charts of hydrological processes and the water vapor budget of depressions over the period of 1979–2002.

Vertical motion and diabatic heating, which were generated by the data assimilation system, were not initially specified. Therefore, the reanalysis vertical motion and diabatic heating issued by the ERA-40 reanalysis may contain bias caused by the spin-up process of the assimilation system. In order to avoid this possible bias, the kinematics method with the O'Brien (1970) adjustment scheme was used to compute the ω fields, and the residual method of the heat budget equation (Chen and Baker, 1986) was applied to generate diabatic heating.

4. Results of analysis

The westward propagation mechanism of monsoon depressions introduced in Section 2 (Fig. 1) includes three basic elements.

(i) A spatial quadrature relationship exists between a monsoon depression depicted by ψ^s and the associated divergent circulation portrayed by χ^s.

(ii) The depression is propagated westward by the negative streamfunction tendency west of the depression center. This streamfunction tendency is generated through the vortex stretching created by the upward branch of the east–west asymmetric circulation across the depression.

(iii) The upward branch of a monsoon depression's east–west circulation coupled with this depression's divergent circulation is maintained by the latent heat released by cumulus convection/rainfall over the depression's west–south-west sector. This convection/rainfall is then rejuvenated by the convergence of water vapor flux driven by the lower-tropospheric divergent circulation.

Budget analyses of heat, water vapor, velocity potential, and streamfunction with all 143 selected monsoon depressions were synthesized to illustrate the westward propagation mechanism, with particular attention focused on the three basic elements of this mechanism listed at the beginning of this section. The major goal of this paper is to present and substantiate the westward propagation mechanism of monsoon depressions, rather than to report the budget analyses in detail. The details of these budget analyses can be found in individual case studies: the heat budget of a MONEX depression (3–8 July 1979) was presented by Saha and Saha (1988), the streamfunction budget of a MONEX depression (5–8 July 1979) was analyzed by Sanders (1984) in terms of the quasi-geostrophic vorticity equation and another MONEX depression (19–25 June 1979) by Chen and Yoon (2000) in terms of the complete vorticity equation, and the water vapor budget of all 143 monsoon depressions during the period 1979–2002 was examined by Yoon and Chen (2005). The only exception is that the velocity-potential maintenance equation (eq. A3) has not been analyzed with any monsoon depression in the past. Because so many depressions were analyzed, composite results during different phases of their life cycles will be presented. The composite procedure of Yoon and Chen (2005) was adopted in this study.

As shown by Chen and Weng (1999, see their fig. 8), the lower-tropospheric summer circulation in south–south-east Asia is characterized by a short-wave train (including three troughs in the Arabian Sea, the Bay of Bengal, and the South China Sea, and two ridges along western India and Indochina) which radiates out of two surface lows over land (the Indian monsoon

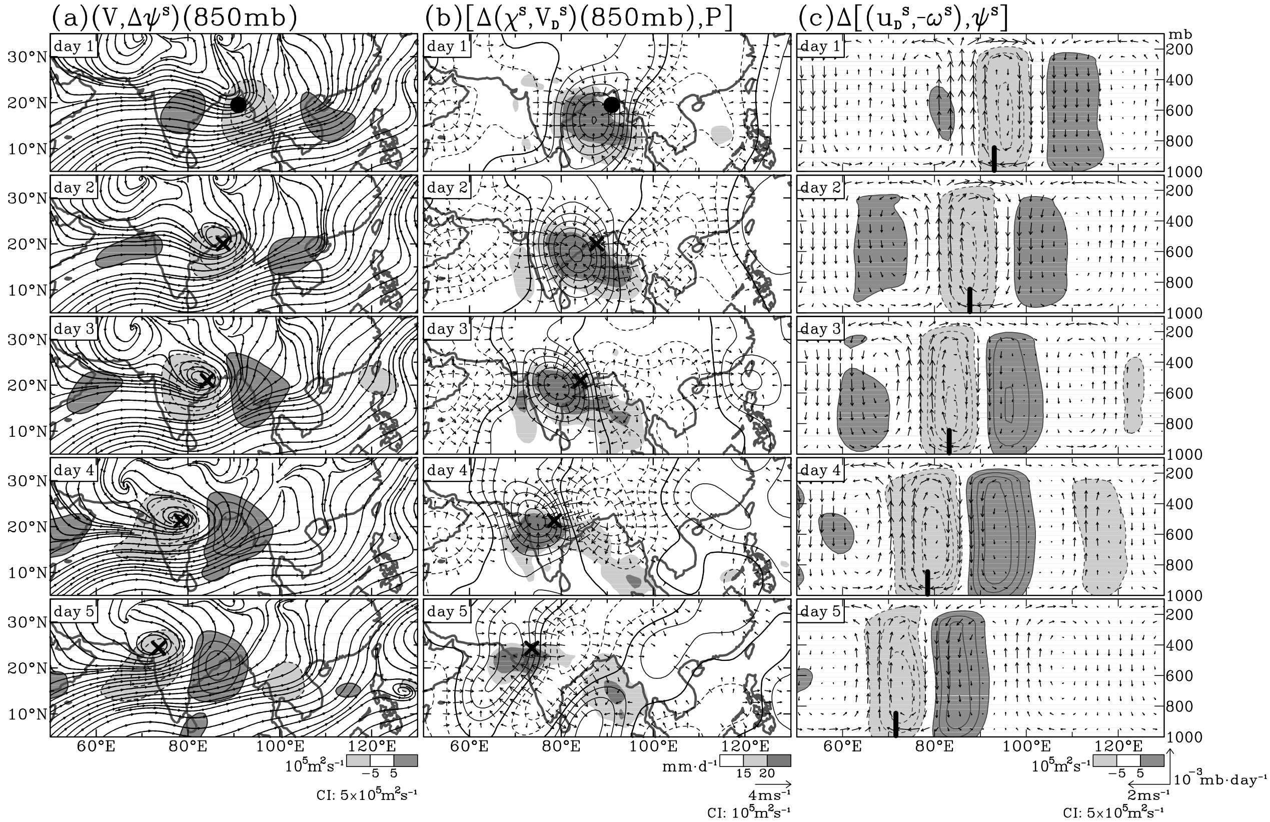

Fig. 2. (a) Composite monsoon depression depicted by the 850-mb streamline field superimposed with streamfunction departures (shaded areas) from their summer (JJA) mean values in the short-wave regime, $\Delta\psi^s$(850 mb), (b) composite 850-mb velocity potential and divergent wind departures in the short-wave regime superimposed with precipitation, $[\Delta(\chi^s, \mathbf{V}_D^s)$ (850 mb), $P]$, and (c) departures of the east–west circulation from their summer-mean values, $\Delta(u_D^s, -\omega^s)$, superimposed with $\Delta\psi^s$ (shaded areas) projected on the longitude–height cross-section cutting through the monsoon depression center. Contour intervals of all variables and measurements of vector lengths are shown at the bottom of each column of figures.

trough and the South China thermal low). In order to avoid obscurity in depicting the horizontal structure of the monsoon depression by the aforementioned stationary short-wave train, the summer-mean value of any variable is removed from composite charts of this variable. For convenience, the departure of any variable, ( ), from its summer-mean value is denoted hereafter by Δ( ). It was revealed from eq. (9) that there should be a spatial quadrature relationship between the ψ^s and χ^s anomalies of a depression. Does such a ψ^s–χ^s spatial relationship really exist? The $\Delta\psi^s$(850 mb) anomalies superimposed on 850-mb streamlines and anomalies of divergent wind vectors $\Delta\mathbf{V}_D^s$ (850 mb) superimposed on the $\Delta\chi^s$(850 mb) anomalies over the depression's life cycle[1] are shown in Figs. 2a and b, respectively. Centers of composite monsoon depression are marked by a dot on day 1 when the depression is formed and a cross thereafter. A spatial quadrature relation emerges between $\Delta\psi^s$(850 mb) and $\Delta\chi^s$(850 mb) anomalies over the entire life cycle of a depression during its westward propagation.

The east–west asymmetrical circulation across a monsoon depression is a part of the depression's divergent circulation. It is thus expected that the east–west circulation anomaly, $\Delta(u_D, -\omega)^s$, on a longitude–height cross-section cutting through the depression center should match with $\Delta\chi^s$(850 mb) during different phases of the depression's life cycle. As shown in Fig. 2c, the upward and downward branches of the east–west circulation are coincident with the corresponding convergent and divergent centers of $\Delta\chi^s$(850 mb) shown in Fig. 2b. Following the divergent circulation of the depression depicted by $\Delta\chi^s$(850 mb), the east–west circulation also propagates westward coherently with the depression (lightly stippled areas in Fig. 2c). The vertical structure of the depression portrayed by $\Delta\psi^s$ seems to be consistent with that depicted by Godbole (1977) in terms of horizontal winds. Nevertheless, a spatial quadrature relationship also exists between the east–west circulation and monsoon depression.

[1]Following Yoon and Chen (2005), the composite life cycle of a depression spans 5 d. Immediately after the depression is formed, the initial stage is designated as day 1. For the next three days, the rainfall of the depression exceeds 25 mm d^{-1}. The life cycle of the depression from days 2 to 4 is defined as the mature phase. The rainfall starts to drop significantly after the mature phase. Therefore, day 5 belongs to the decaying phase.

In view of this spatial quadrature relationship between $\Delta\psi^s$(850 mb) and $\Delta\chi^s$(850 mb) and between $\Delta\psi^s$ and $\Delta(u^s_D, -\omega^s)$, the following two questions are raised

(i) How is the divergent circulation of a monsoon depression maintained?

(ii) What is the dynamic implication of the spatial quadrature relationship between $\Delta\psi^s$ and $\Delta\chi^s$ of a monsoon depression? How is this spatial quadrature ψ^s–χ^s relationship maintained?

Let us first explore the answer to the first question. As inferred from eqs. (3) and (4), rainfall in the west–south-west sector of a depression should be maintained by the convergence of water vapor flux toward this region generated by the depression's divergent circulation. The $[\Delta(\chi^s_Q, \mathbf{Q}^s_D), P]$ fields during different phases of the depression are shown in Fig. 3 (adopted from fig. 4b of Yoon and Chen, 2005). Comparing $\Delta(\chi^s_Q, \mathbf{Q}^s_D)$ to $\Delta(\chi^s, V^s_D)$(850 mb) in Fig. 2b, similar spatial patterns between these two fields during different phases of a depression life cycle confirm our inference. In addition to supporting the rainfall of a depression, how does the feedback of the latent heat released by cumulus convection/rainfall maintain a divergent circulation? It is inferred from eq. (1) that the east–west circulation of a depression is driven by the latent heat released in the west–south-west sector of a depression. This inference is confirmed by coincident patterns of $-\Delta\omega^s$(500 mb) and $\Delta\dot{\mathbf{Q}}^s$(500 mb) shown in Figs. 4a and b, respectively: upward (downward) motion west (east) of the depression coincides with heating (cooling). To support this argument further, the east–west circulation superimposed with diabatic heating projected on the longitude–height cross-section through the center of a depression $[\Delta(u^s_D, -\omega^s), \Delta\dot{\mathbf{Q}}^s]$ is shown in Fig. 4c. The in-phase relationship between diabatic heating and vertical motion is reflected by the coincidence of heating (cooling) with the upward (downward) branch of the east–west circulation. Because the east–west circulation is a part of the divergent circulation, it is also expected that the divergent circulation should be maintained by adiabatic heating. This argument is supported by a comparison between $[\Delta(\chi^s_{\dot{Q}}, \mathbf{V}^s_D)$ (850 mb), $\Delta\langle\dot{\mathbf{Q}}\rangle^s]$ in Fig. 5 (where $\langle\ \rangle = (1/p)\int_0^{ps}\langle\ \rangle\,\mathrm{d}p$) and $\Delta(\chi^s, \mathbf{V}^s_D)$(850 mb) in Fig. 2b. It was found from the heat budget analysis that local temperature change $(\partial T/\partial t)$ and thermal advection $(-\mathbf{V}\cdot\nabla T)$ are generally much smaller than adiabatic warming and diabatic heating. The magnitude and spatial structure of $\Delta\chi^s_{\dot{Q}}$ and $\Delta\chi^s$ should be close to each other. Actually, Variance$[\Delta\chi^s_{\dot{Q}}$(850 mb)]/Variance$[\Delta\chi^s$(850 mb)] shown in Fig. 5 is always larger than or equal to 99% over the entire life cycle of a depression. It is revealed from such a large variance ratio that the depression's divergent circulation is primarily driven by diabatic heating.

We demonstrated previously that the rainfall of a monsoon depression was supported by convergence of water vapor transported by the lower-tropospheric divergent circulation of a depression. Next, we argued that divergent circulation/east–west circulation of a depression could be maintained by the latent heat released by cumulus convection/rainfall. It becomes obvious that there is a feedback interaction between rainfall and the divergent circulation of a depression. However, what is the dynamic role played by this feedback interaction in the westward propagation of a depression? The answer to this question in terms of the streamfunction budget eq. (4) is identical to answering the second question raised above. Results of the $\Delta\psi^s$(850 mb) budget analysis are presented in Fig. 6.

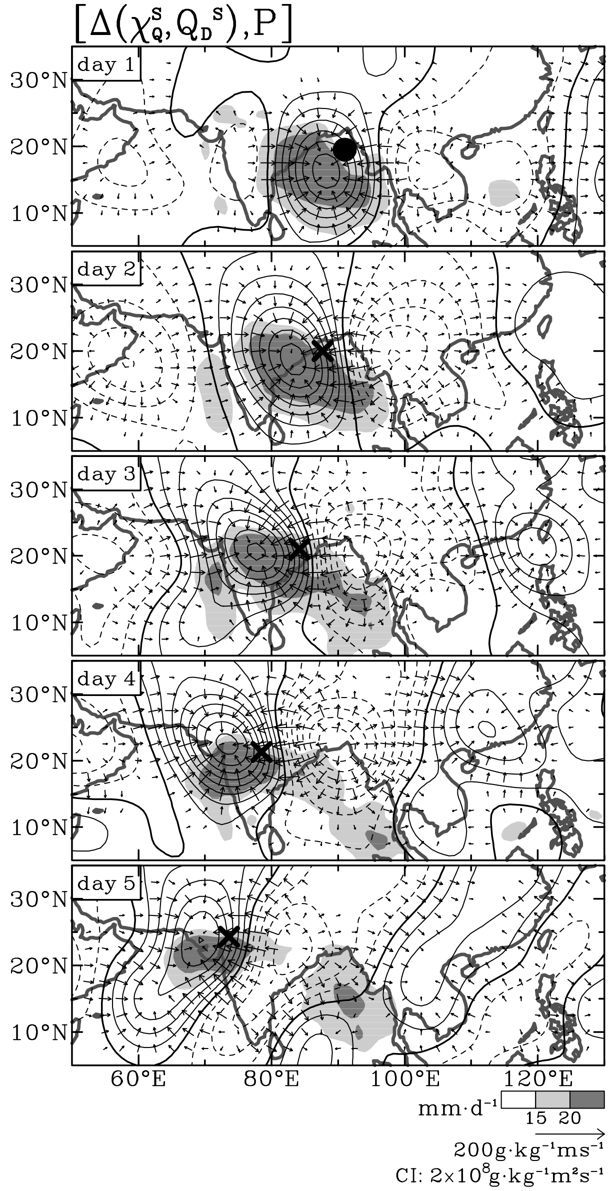

Fig. 3. Same as Fig. 2b, except for $[\Delta(\chi^s_Q, \mathbf{Q}^s_D), P]$.

As shown in Fig. 6, $\Delta\psi^s_A$(850 mb) and $\Delta\psi^s_\chi$(850 mb) are spatially in quadrature with the $\Delta\psi^s$(850 mb) anomalies (shaded areas in Fig. 6) of the composite monsoon depression. The

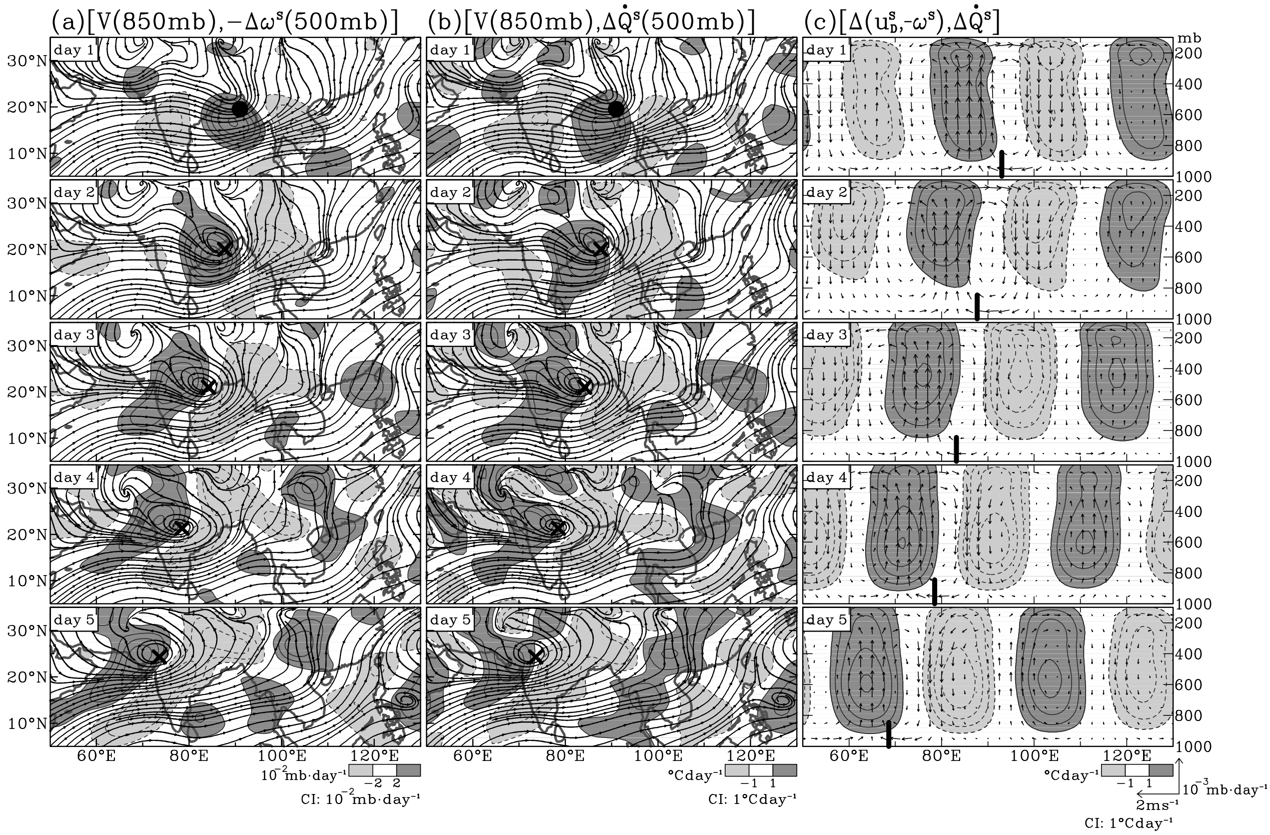

Fig. 4. Composite 850-mb streamline charts superimposed with departures of (a) p vertical velocity, $-\Delta\omega^{s}$, (b) diabatic heating, $\Delta\dot{\mathbf{Q}}^{s}$, and (c) east–west circulation, $\Delta(u^{s}_{D}, -\omega^{s})$, superimposed with $\Delta\dot{\mathbf{Q}}^{s}$, from their summer-mean values. Depression centers in different phases of its life cycle are marked by dots, crosses, and sticks. Contour intervals of different variables are shown at the bottom of each column of figures.

streamfunction tendency, $\Delta\psi^{s}_{t}$(850 mb), should be generated by the combination of these two dynamic processes. Note that the magnitude of $\Delta\psi^{s}_{\chi}$ (850 mb) is much larger than that of $\Delta\psi^{s}_{A}$ (850 mb), as observed in the streamfunction budget of a MONEX depression by Chen and Yoon (2000). This comparison enables us to reach the following approximation

$$\Delta\psi^{s}_{t}(850\,\text{mb}) \sim \Delta\psi^{s}_{\chi}(850\,\text{mb}). \tag{10}$$

Based on the composite $\Delta\psi^{s}$(850 mb) budget of monsoon depressions, it is clear that $\Delta\psi^{s}_{A}$(850 mb) (streamfunction tendency generated by total vorticity advection) is not an effective dynamic process in generating $\Delta\psi^{s}_{t}$(850 mb). Instead, $\Delta\psi^{s}_{\chi}$(850 mb) coupled with the east–west asymmetric circulation of the monsoon depression is the primary dynamic process in propagating a monsoon depression westward. According to eq. (9), the dynamic relationship of eq. (10) requires a spatial quadrature relationship between divergent circulation ($\Delta\chi^{s}$)/east–west circulation $\Delta(u^{s}_{D}, -\omega^{s})$ and the westward propagating monsoon depressions ($\Delta\psi^{s}$). Budget analyses of heat, water vapor, velocity potential, and streamfunction lead us to conclude that the westward propagation of monsoon depressions is a result of the feedback interaction between cumulus convection/rainfall and divergent circulation coupled with the dynamical interaction between the divergent circulation and monsoon depression.

Up to this point, the westward propagation of monsoon depressions and their spatial $\Delta\psi^{s}$–$\Delta\chi^{s}$ quadrature relationship are explained in terms of eq. (6). However, this dynamic relationship does not explain why the upward branch of the east–west asymmetric circulation and rainfall/cumulus convection occur in the west–south-west sector of monsoon depressions. It was found by Chen and Yoon (2000) in their streamfunction budget analysis of a MONEX depression that prior to/during the depression formation (i.e. day $-2 \sim 1$), meridional advection of total vorticity was larger than zonal advection of relative vorticity

$$\left[-v\frac{\partial}{\partial y}\left(f - \frac{\partial u}{\partial y}\right)\right] > \left[-u\frac{\partial \zeta}{\partial x}\right]$$

over the west–south-west sector of the depression. During this stage of a depression, the meridional shear of monsoon westerlies is often positive/cyclonic south of the maximum westerlies. Streamfunction tendencies generated by these advections of vorticity are represented by $\psi^{s}_{Ay+A\beta}$ and ψ^{s}_{Ax}, respectively, as shown in Fig. 7. At this stage, the zonal advection of relative vorticity $[-u(\partial\zeta/\partial x)]$ is much smaller than the meridional advection of total vorticity. This positive meridional advection

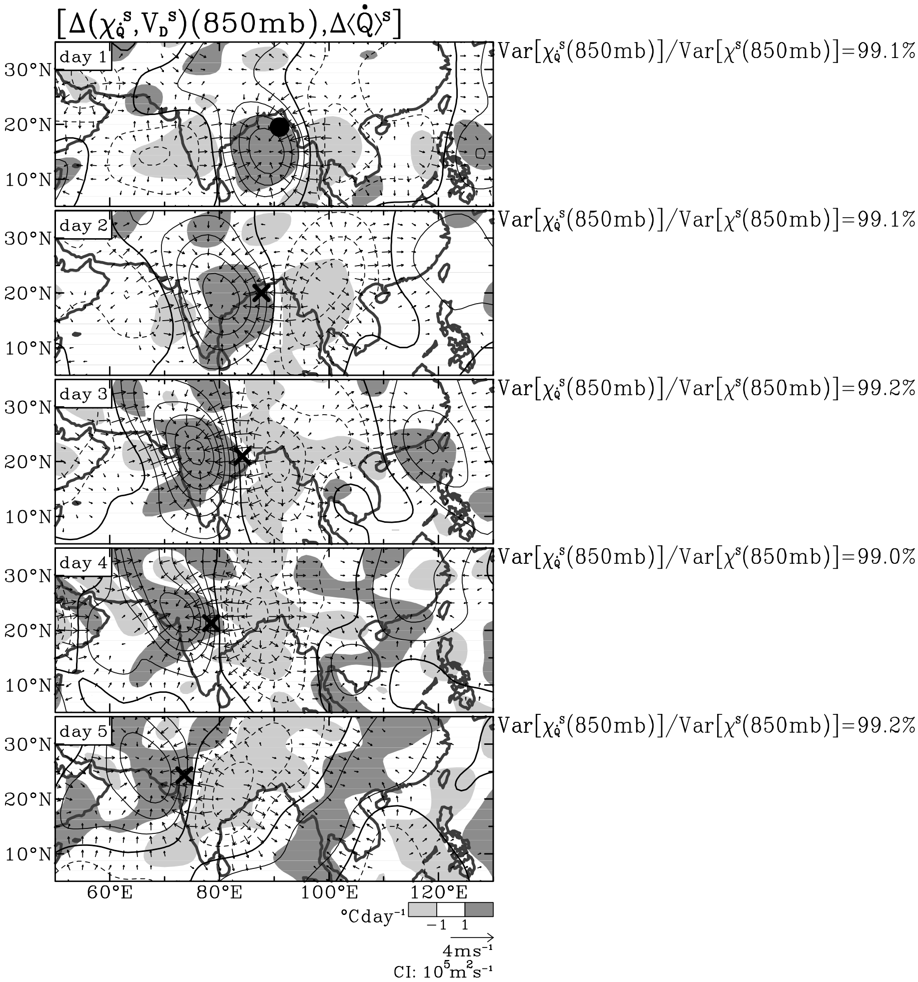

Fig. 5. Same as Fig. 2b, except for $[\Delta(\chi^{s}_{\dot{Q}}, \mathbf{V}^{s}_{D})\,(850\,\mathrm{mb}), \Delta\langle\dot{\mathbf{Q}}\rangle^{s}]$, where $\langle\ \rangle \equiv (1/p_s)\int_0^{p_s}\langle\ \rangle\,dp$.

of total vorticity (which generates negative streamfunction tendency) over the west–south-west sector of monsoon depressions initiates upward motion and the east–west asymmetric circulation. After this circulation is formed, the feedback interaction between rainfall/cumulus convection over the west–south-west sector of a monsoon depression and the divergent circulation is coupled with the dynamic process, ψ^{s}_{χ}, in maintaining the westward propagation of the depression and the spatial quadrature ψ^{s}–χ^{s} relationship. This argument can be confirmed by the contrast between $\psi^{s}_{A}(850\ \mathrm{mb})$ and $\psi^{s}_{\chi}(850\ \mathrm{mb})$ at day 1 in Fig. 6.

5. Concluding remarks

The Saha and Saha (1988) heat budget analyses of a MONEX monsoon depression suggested the possible existence of an east–west asymmetric circulation across a monsoon depression. On the other hand, the streamfunction budget of individual monsoon depressions by Sanders (1984) and Chen and Yoon (2000) showed that advection of total vorticity was negligible in the westward propagation of monsoon depressions. Indeed, the streamfunction tendency generated by vortex stretching over the west–south-west sector of a monsoon depression is vital to its westward propagation. It was shown in a recent study by Yoon and Chen (2005) that rainfall in the west–south-west sector of a depression was maintained by convergence of water vapor flux driven by the depression's east–west circulation. Major findings of previous studies lead us to introduce a westward propagation mechanism of monsoon depressions depicted by a schematic diagram shown in Fig. 1. A monsoon depression is propagated westward by the negative streamfunction tendency west of the depression, which is generated through vortex stretching by the upward branch of a depression's east–west circulation. This upward branch is maintained by the latent heat released from rainfall over the west–south-west sector of the depression. Based on the feedback interaction between diabatic heating and the east–west circulation/divergent circulation and the dynamic coupling between the divergent circulation and the monsoon depression through vortex stretching, a link between diabatic heating and

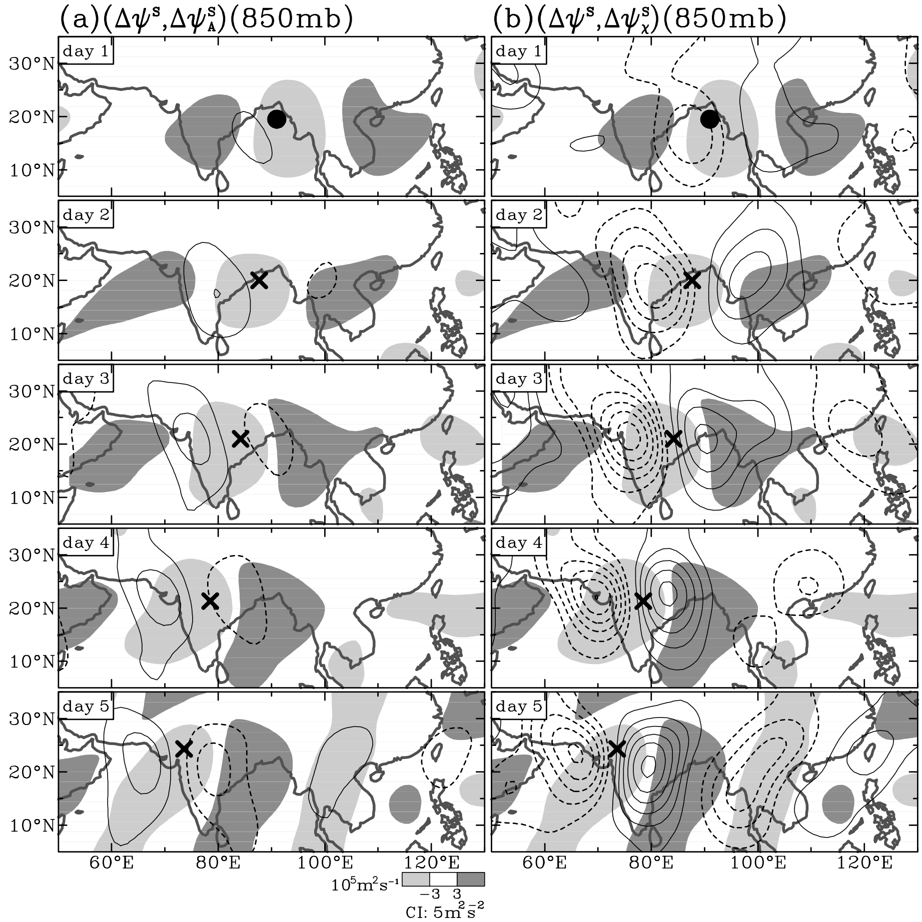

Fig. 6. Departures of 850-mb streamfunction (shaded areas), $\Delta\psi^s$ (850 mb), superimposed with departures of 850-mb streamfunction tendencies generated by (a) total vorticity advection, $\Delta\psi^s_A$ (850 mb), and (b) vortex stretching, $\Delta\psi^s_\chi$ (850 mb). Contour intervals of $\Delta\psi^s$ (850 mb) and streamfunction tendencies $\Delta\psi^s_A$ and $\Delta\psi^s_\chi$ are shown at the bottom of the left column.

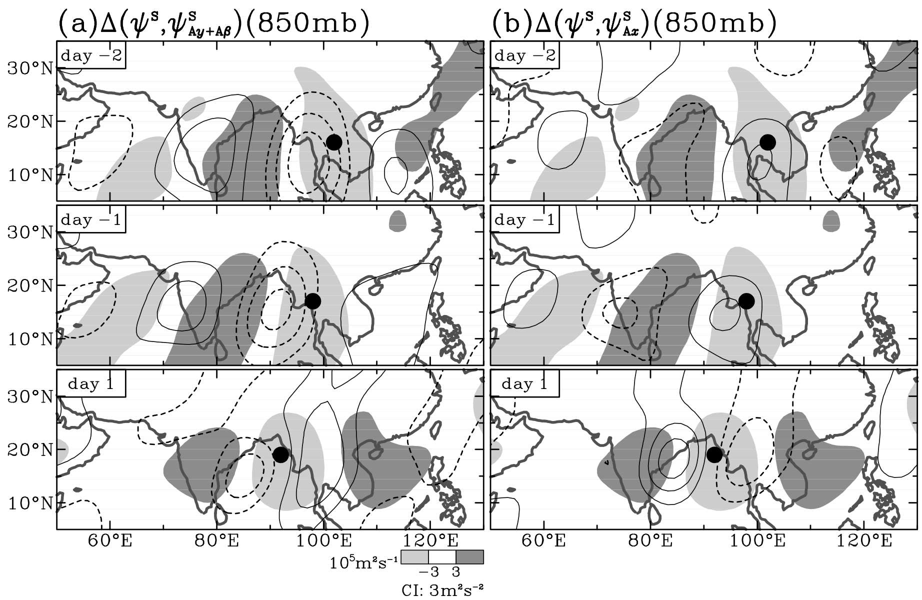

Fig. 7. Same as Fig. 6, except for $\Delta\psi^s_{Ay+A\beta}$ (850 mb) and $\Delta\psi^s_{Ax}$ (850 mb).

divergent circulation should be established. The velocity potential maintenance equation (Chen and Yen, 1991a,b) was used to serve this purpose.

Except for the water vapor budget analysis of depressions presented recently by Yoon and Chen (2005), the Saha and Saha (1988) heat budget analysis and the streamfunction budget analyses of Sanders (1984) and Chen and Yoon (2000) focused only on individual monsoon depressions. In this study, budget analyses of heat, water vapor, streamfunction, and velocity potential were performed for all 143 monsoon depressions identified by Yoon and Chen (2005). The westward propagation mechanism of monsoon depressions presented by the schematic diagram in Fig. 1 could be elucidated by results of these comprehensive budget analyses over the composite life cycle of depressions in terms of the ERA-40 reanalysis and three sets of daily global satellite-gauge observed precipitation. The westward propagation mechanism of monsoon depressions not only discloses the cause of this peculiar propagation behavior, but also facilitates the improvement in forecasts of these depressions.

The tropical atmosphere is conditionally unstable (e.g. Riehl, 1979). Therefore, convection may be triggered by an uplift of air parcel forced by the low-level convergence of a synoptic disturbance. The divergent circulation embedded by this convergence may be intensified/maintained by the latent heat released from cumulus. This feedback interaction also develops the tropical synoptic disturbance through vortex stretching. Most tropical disturbances, which are transported by tropical easterlies, are developed by this CISK mechanism. In contrast, the westward propagating depressions are embedded in the monsoon westerlies within the Indian monsoon trough and overlaid by the Tibetan high. The feedback interaction between diabatic heating and divergent circulation functions in a way like the CISK mechanism. The westward propagation of a depression by the negative streamfunction tendency generated through vortex stretching by the east–west asymmetric circulation across a depression differs from the traditional wave-CISK mechanism of tropical disturbances (e.g. Hayashi, 1970; Lindzen, 1974, and many others). Except for monsoon depressions, synoptic disturbances in the tropics do not propagate under any major tropical anticyclone in the upper troposphere. These distinctions between monsoon depressions and other tropical disturbances strongly suggest that the wave-CISK-like mechanism of monsoon depression's westward propagation should be further tested by analytic analysis and numerical simulations with simple models forced by a medium-deep cumulus convection scheme.

As pointed out earlier, half of the Indian monsoon rainfall is produced by monsoon depressions. Thus, the weather prediction of monsoon depressions is important to human activity on the Indian subcontinent. In order to accurately predict the intensity, propagation, and rainfall of a depression, basic elements of the Indian monsoon circulation (including the Tibetan high, the monsoon trough, and monsoon westerlies) should be properly simulated. However, the water vapor supply and rainfall are important to maintain the east–west circulation, and, in turn, to determine the westward propagation speed of monsoon depressions. Therefore, cumulus convection schemes, which were not developed to simulate convection in the monsoon environment, have to be properly designed in such a way that they can handle medium-depth convection capable of generating heavy rainfall underneath the Tibetan high.

6. Acknowledgements

This study is supported by the National Science Foundation Grant ATM-0434798. Comments offered by two anonymous reviews were very helpful in improving the presentation of this paper. The editing assistance of Mr Dave Flory is appreciated.

7. Appendix A: Budget equations of heat, water vapor, velocity potential and streamfunction

The budget equations used in this study are: the heat equation

$$\frac{\partial T}{\partial t} + \mathbf{V}\cdot\nabla T - \sigma\omega = \frac{1}{c_{\mathrm{p}}}\dot{\mathbf{Q}}; \quad \text{(A1)}$$

the water vapor equation

$$\frac{\partial W}{\partial t} + \nabla\cdot\mathbf{Q} = E - P; \quad \text{(A2)}$$

the velocity potential-maintenance equation, which is obtained by combing the continuity equation and thermal equations

$$\chi = \nabla^{-2}\left\{\frac{\partial}{\partial p}\left[\frac{1}{\sigma}\left(\frac{\partial T}{\partial t} + \mathbf{V}\cdot\nabla T\right)\right]\right\} + \nabla^{-2}\left[\frac{\partial}{\partial p}\left(\frac{-1}{\sigma c_{\mathrm{p}}}\dot{Q}\right)\right]$$

$$\chi_{\mathrm{t}} \qquad \chi_H \qquad \chi_Q; \quad \text{(A3)}$$

and the streamfunction budget equation, which is the Laplace inverse transform of the vorticity equation

$$\nabla^{-2}\left(\frac{\partial\zeta}{\partial t}\right) = \nabla^{-2}\left[-\mathbf{V}\cdot\nabla(\zeta+f)\right] + \nabla^{-2}\left[-(\zeta+f)\nabla\cdot\mathbf{V}\right]$$

$$\psi_{\mathrm{t}} \qquad \psi_{\mathrm{A}} \qquad \psi_{\chi}. \quad \text{(A4)}$$

The notation used is conventional. Symbols used are explained in Table 1.

References

Burpee, R. W. 1972. The origin and structure of easterly waves in the lower troposphere of North Africa. *J. Atmos. Sci.* **29**, 77–90.

Carlson, T. N. 1969a. Synoptic histories of three African disturbances that developed into Atlantic hurricanes. *Mon. Wea. Rev.* **97**, 256–276.

Carlson, T. N. 1969b. Some remarks on African disturbances and their progress over the tropical Atlantic. *Mon. Wea. Rev.* **97**, 716–726.

Chen, T-C. 1985. Global water vapor flux and maintenance during FGGE. *Mon. Wea. Rev.* **113**, 1801–1819.

Chen, T-C. and Baker, W. E. 1986. Global diabatic heating during SOP-1 and SOP-2. *Mon. Wea. Rev.* **114**, 2776–2790.

Chen, T-C. and Weng, S-P. 1999. Interannual and intraseasonal variations in monsoon depressions and their westward-propagating predecessors. *Mon. Wea. Rev.* **127**, 1005–1020.

Chen, T-C. and Yen, M-C. 1991a. Interaction between intraseasonal oscillations of the midlatitude flow and tropical convection during 1979 northern summer: the Pacific Ocean. *J. Climate* **4**, 653–671.

Chen, T-C. and Yen, M-C. 1991b. A study of the diabatic heating associated with the Madden–Julian Oscillation. *J. Geophys. Res.* **96**, 13163–13177.

Chen, T-C. and Yoon, J.-H., 2000. Some remarks on the westward propagation of the monsoon depression. *Tellus* **52A**, 487–499.

Cressman, G. P. 1957. An operational objective analysis system. *Mon. Wea. Rev.* **87**, 367–374.

Daggupaty, S. M. and Sikka, D. R. 1977. On the vorticity budget and vertical velocity distribution associated with the life cycle of a monsoon depression. *J. Atmos. Sci.* **34**, 773–792.

Godbole, R. V. 1977. The composite structure of the monsoon depression. *Tellus* **29**, 25–40.

Hayashi, Y. 1970. A theory of large-scale equatorial waves generated by condensation heat and accelerating the zonal wind. *J. Meteorol. Soc. Japan* **48**, 140–160.

Huffman, G. J., Adler, R. F., Arkin, P., Chang, A., Ferraro, R. and coauthors. 1997. The Global Precipitation Climatology Project (GPCP) combined precipitation data set. *Bull. Am. Meteorol. Soc.* **78**, 5–20.

Källberg, P., Simmons, A., Uppala, S. and Fuentens, M. 2004. The ERA-40 archive. *ERA-40 Project Report Series No. 17*. Available online at http://www.ecmwf.int/publications/

Krishnamurti, T. N., Molinari, J., Pan, H. and Wong, V. 1977. Downstream amplification and formation on monsoon disturbances. *Mon. Wea. Rev.* **105**, 1281–1297.

Lindzen, R. S. 1974. Wave-CISK in the tropics. *J. Atmos. Sci.* **31**, 156–179.

Matsuno, T. 1966. Quasi-geostrophic motions in the equatorial area. *J. Meteorol. Soc. Japan* **53**, 227–240.

O'Brien, J. J. 1970. Alternative solution to the classic vertical velocity problem. *J. Appl. Meteorol.* **9**, 197–203.

Palmer, C. P. 1952. Tropical meteorology. *Q. J. R. Meteorol. Soc.* **78**, 126–163.

Reed, R. J. and Recker, E. E. 1971. Structure and properties of synoptic wave disturbances in the equatorial western Pacific. *J. Atmos. Sci.* **28**, 1117–1133.

Riehl, H. 1954. *Tropical Meteorology*. McGraw-Hill, New York, 392 pp.

Riehl, H. 1979. *Climate and Weather in the Tropics*. Academic Press, 611 pp.

Saha, K. and Saha, S. 1988. Thermal budget of a monsoon depression in the Bay of Bengal during FGGE-MONEX 1971. *Mon. Wea. Rev.* **116**, 242–254.

Saha, K., Sanders, F. and Shukla, J. 1981. Westward propagating predecessors of monsoon depressions. *Mon. Wea. Rev.* **109**, 330–343.

Sanders, F. 1984. Quasi-geostrophic diagnosis of the monsoon depression of 5–8 July 1979. *J. Atmos. Sci.* **41**, 538–552.

Shukla, J. 1978. CISK-barotropic-baroclinic instability and the growth of monsoon depressions. *J. Atmos. Sci.* **35**, 495–508.

Sikka, D. R. 1977. Some aspects of the life history, structure, and movement of monsoon depressions. *Pageoph* **115**, 1501–1529.

Simpson, J., Adler, R. F. and North, G. R. 1988. A proposed Tropical Rainfall Measuring Mission (TRMM) satellite. *Bull. Am. Meteorol. Soc.* **69**, 278–295.

Susskind, J., Piraino, P., Rokke, L., Iredell, L. and Mehta, A. 1997. Characteristics of the TOVS Pathfinder Path A Data Sets. *Bull. Am. Meteorol. Soc.* **78**, 1449–1472.

Yanai, M., Maruyama, T., Nitta, T. and Hayashi, Y. 1968. Power spectra of large-scale disturbances over the tropical Pacific. *J. Meteorol. Soc. Japan* **46**, 308–323.

Yoon, J-H. and Chen, T.-C., 2005. Water vapor budget of the Indian monsoon depression. *Tellus* **57A**, 770–782.